The water-bag distribution function for kinetic modeling

E. Gravier[1], P. Morel[1], R. Klein[1], N. Besse[1], J. H. Chatenet[1], P. Bertrand[1], X. Garbet[2]

[1]*Institut Jean Lamour, UMR 7198 CNRS-Université, Nancy, France*

[2]*CEA - IRFM, Association Euratom-CEA, Cadarache, France*

Predicting turbulent transport in nearly collisionless fusion plasmas can be solved by using gyrokinetic equations [1] but is still a nontrivial task because of its demand of computer resources. This motivated us to revisit an alternative approach based on the water-bag (WB) representation of the distribution function. The nonlinear behavior of a system is often determined more by the over-all structure of the distribution function than by its precise details. It can be useful to choose for the distribution function f a step function, called a water-bag function, that consists of a finite number of regions of f constant (Fig. 1). According to Liouville's phase-space conservation property the distribution function remains constant in time between the regions. The state of the system is then completely defined by specifying the boundary curves (contours, see Fig. 2) between the different regions, allowing one to keep the kinetic aspect of the problem with the same complexity as a multifluid model.

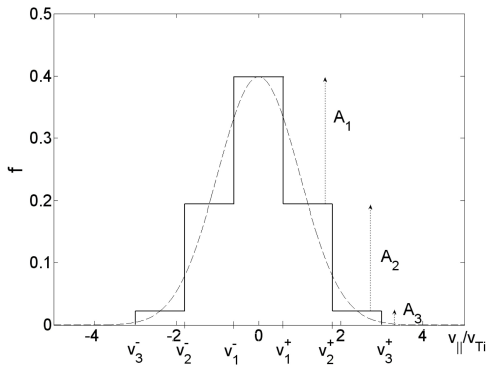

FIGURE 1 – Water-bag distribution function for $M = 3$ bags plotted against the parallel velocity.

Introduced initially by DePackh [2], this model was extended in magnetized plasmas in the framework of gyrokinetic modeling, first in cylindrical geometry with a uniform and static magnetic field pointing in the axis direction. A linear study of the ion temperature gradient (ITG) instability in cylindrical geometry has been performed [3]. It allowed us to obtain the following differential equation :

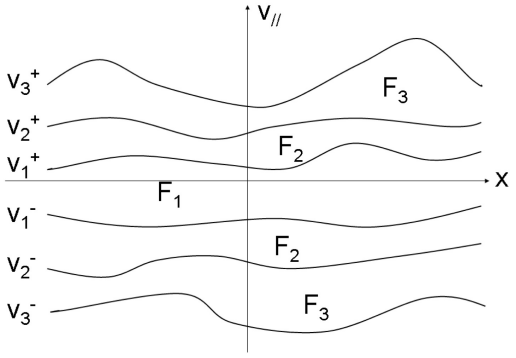

FIGURE 2 – Bag contours in the phase space $x - v$ for a three-bag system.

$$\frac{d^2\phi}{dr^2} + \left(\kappa_n + \frac{1}{r}\right)\frac{d\phi}{dr} + \left[Q(r) - k_\theta^2\right]\phi = 0 \quad (1)$$

where

$$Q(r) = \frac{J_0^2}{r_{Li}^2}\left(\sum_{j=1}^{M}\alpha_j \frac{k_\parallel^2 v_{Ti}^2 - \omega\Omega_j^\star}{\omega^2 - k_\parallel^2 a_j^2}\right) - \frac{1}{Z_i^\star r_{Li}^2} \tag{2}$$

ϕ is the amplitude of the perturbed plasma potential, $\kappa_n = \partial_r \ln n_0(r)$, the poloidal wave number is $k_\theta = m/r$ where m is the mode number, J_0 is the gyroaverage operator, r_{L_i} is the ion Larmor radius, v_{T_i} is the ion thermal velocity, M is the bag number, a_j is the j^{th} bag velocity at the equilibrium, ω is the frequency of the perturbation, α_j is the j^{th} bag relative ion density, $\Omega_j^\star = \frac{k_B T_i}{qB} k_\theta \partial_r \ln a_j(r)$, $k_\parallel$ is the parallel wave number and $Z_i^\star = \frac{T_e}{T_i}\frac{q}{e}$.

In the simplest case where ϕ is constant it has been shown that the water-bag model converges rather rapidly towards that of the continuous distribution function when ITG instability threshold and linear growth rates are compared (Fig. 3). Indeed, analyzing the dependence of the linear growth rate on the bag number for $\Omega_n^\star = -1.0$ and $\Omega_T^\star = -8.0$ (in $k_\parallel v_{Ti}$ unit, see Fig. 3) shows that the instability growth rate reaches respectively 93% and 98.5% of its continuous rate (bag number $\to \infty$) for 5 and 10 bags, whereas the fluid model overestimates the continuous kinetic rate by a factor equal to 1.6.

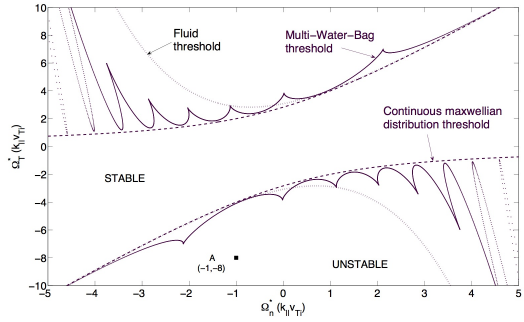

FIGURE 3 – ITG instability threshold plotted against $\Omega_n^\star$ and $\Omega_T^\star$ for 10 bags.

Quasilinear and nonlinear numerical simulations of ITG instabilities have also been carried out in cylindrical geometry [4]. As a result, the quasilinear approach proves to be a good approximation of the full nonlinear gyro-water-bag.

Next, a local linear study of multi-species effects on ITG instability has been performed [5] (Fig. 4). Each ion species is modeled via a multi-water-bag distribution function. Here we focused on the case of a plasma composed of deuterium and carbon. $\kappa_{T_d} = \partial_r \ln T_d = -10 k_\parallel$ and the carbon density is 10 % of the deuterium density. The impact of the carbon density gradient on the linear stability of the plasma has been studied. The stability threshold strongly depends on the ratio between deuterium and carbon radial density gradients (Fig. 4). The κ_{n_d} range in which the plasma is unstable is wider in the

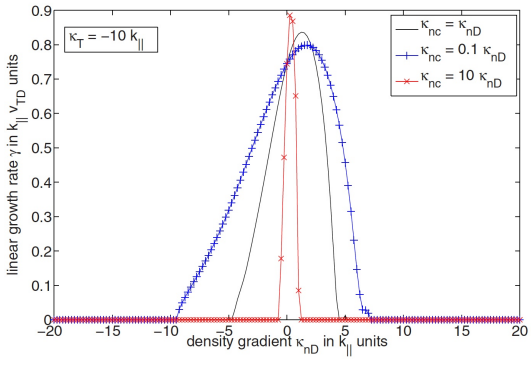

FIGURE 4 – ITG linear growth rate plotted against deuterium κ_n for three different density peaking of carbon.

case of a low carbon density gradient ($\kappa_{n_c} = 0.1\kappa_{n_d}$) than in the case of higher carbon density gradients ($\kappa_{n_c} = 10.0\kappa_{n_d}$). The density peaking of impurity decreases the width of the unstable area while it increases its maximum value.

Next the water-bag model has been used to study finite Larmor radius effects with the possibility of using the full Larmor radius distribution instead of an averaged Larmor radius [6]. The main result is that the accurate magnetic moment distribution is needed to correctly describe plasma instabilities when the distribution function is not a Maxwellian one. As an example of non-Maxwellian distribution function, a bi-Maxwellian one was considered. This case corresponds to an energetic population immersed in a core plasma. The instability growth rate decreases as the fraction of energetic ions increases (Fig. 5). The full treatment of the Larmor radius effect (dotted line) yields a greater instability growth rate when compared to the averaged Larmor radius case (solid line).

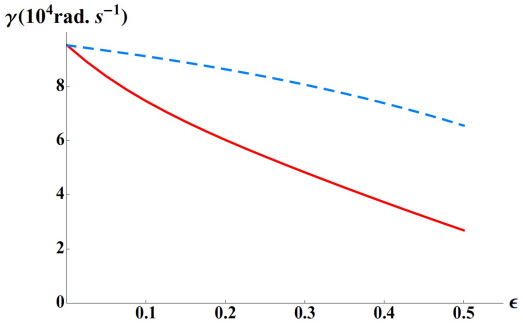

FIGURE 5 – ITG linear growth rate plotted against the fraction ε of energetic particles in the plasma.

Moreover, a linear study of both collisional drift waves and ITG instabilities has been performed in the case of a linear magnetized plasma [7]. Electron-neutral collisions are now taken into account. In the case of a strong magnetic field ion-neutral collisions and their stabilizing effect are neglected. Consequently an ion water-bag distribution function is used. Kinetic effects on collisional drift waves have been investigated (Fig. 6). With T_e and T_i equal to 2 eV the expected phase velocity is of the order of the ion thermal velocity, allowing particle-wave interactions. The one-bag case is equivalent to a fluid model and the 20-bag case is equivalent to a kinetic model. As expected fluid and kinetic models do not give the same results. Indeed the kinetic phenomena play a stabilizing role when the thermal velocity is close to the phase velocity. In both cases the $m = 2$ mode is the most unstable but the linear growth rate given by the kinetic model is significantly lower than that of given by a fluid model (see Fig. 6). Also the transition from collisional drift waves to ITG

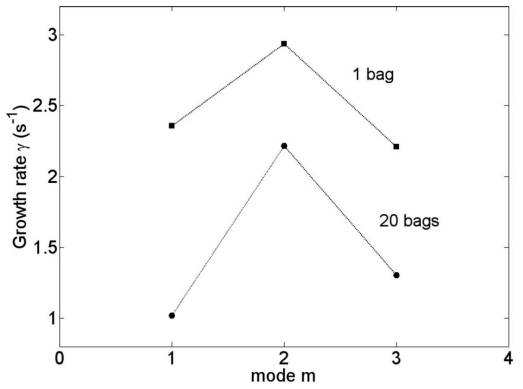

FIGURE 6 – Drift waves instability growth rate plotted against the mode m.

instability depending on the ion temperature gradient has been studied (Fig. 7).

Finally first linear results in toroidal geometry have shown the capability of this WB model in describing ITG instabilities in toroidal geometry [8]. The curvature effects of the magnetic field have been investigated. After some assumptions a linear eigenvalue equation has been derived and solved in the case of a local linear analysis (Fig. 8). For comparison ITG instability growth rate in cylindrical geometry is shown. As expected the disturbances are all the more unstable that the gradient of the plasma pressure and that of the magnetic field are of the same sign. The maximum linear growth rate is located at the low field side of the torus ($\theta = 0$). This property is very well recovered in the case of the interchange instability, for which the growth rate is zero at the strong field side ($\theta = \pm\pi$).

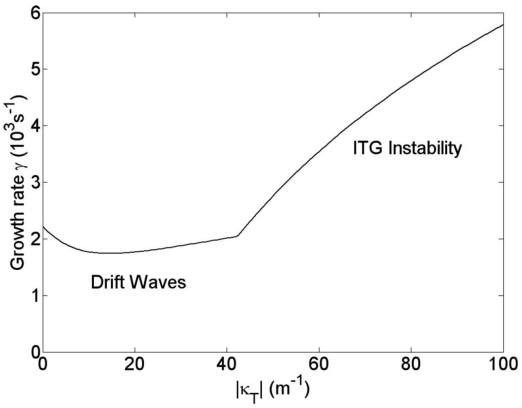

FIGURE 7 – Transition from collisional drift waves to ITG instability. The growth rate of the most unstable mode is plotted against the parameter $\kappa_T = \partial_r \ln T_i$.

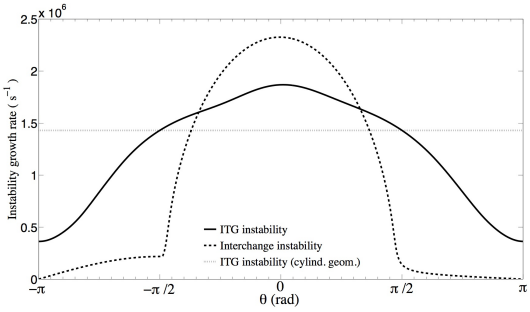

FIGURE 8 – ITG ($k_{\|} \neq 0$) and interchange ($k_{\|} = 0$) instability growth rates plotted against the poloidal angle θ in toroidal geometry.

Références

[1] T. S. Hahm, Phys. Fluids, **31**, 2670 (1988)

[2] D. C. DePackh, J. Electron. Control, **13**, 417 (1962)

[3] P. Morel, E. Gravier, N. Besse, R. Klein, A. Ghizzo, P. Bertrand, X. Garbet, P. Ghendrih, V. Grandgirard and Y. Sarazin, Phys. Plasmas, **14**, 112109 (2007)

[4] N. Besse, P. Bertrand, P. Morel and E. Gravier, Phys. Rev. E, **77**, 056410 (2008)

[5] P. Morel, E. Gravier, N. Besse, R. Klein, A. Ghizzo, P. Bertrand, C. Bourdelle and X. Garbet, Phys. Plasmas, **18**, 032512 (2011)

[6] R. Klein, E. Gravier, P. Morel, N. Besse and P. Bertrand, Phys. Plasmas, **16**, 082106 (2009)

[7] E. Gravier, R. Klein, P. Morel, N. Besse and P. Bertrand, Phys. Plasmas, **15**, 122103 (2008)

[8] R. Klein, E. Gravier, J. H. Chatenet, N. Besse, P. Bertrand and X. Garbet, EPJ D (2011)